Environ Sci Pollut Res (2017) 24:13184–13202
DOI 10.1007/s11356-016-8087-x

Hydrogeochemical characterization of the thermal springs in northeastern of Los Cabos Block, Baja California Sur, México

Pablo Hernández-Morales[1] · **Jobst Wurl**[1]

Received: 1 July 2016 / Accepted: 9 November 2016 / Published online: 19 November 2016

Abstract The existence of hot springs in the northeastern part of Los Cabos Baja California Sur (BCS), is known from pre-Hispanic times, but their hydrochemical composition had not been previously described. Several springs are located within the watershed of Santiago, and the objective of this study was to define the hydrogeochemical composition of the thermal springs and to characterize the geothermal reservoir. A total of 16 water samples were taken in 11 geothermal manifestations under dry (June 2014) and humid (March 2015) conditions. A geothermal system of low enthalpy and low mineralization was found along the San José del Cabo Fault (FSJC), with an average salinity (TDS) of 261 mg/L and an alkaline pH (8.5–9.5). The hydrogeochemical composition corresponds to the sodium-bicarbonate type, and geothermometers (silica and Na–K) indicate temperatures ranging from 70 to 115 °C for the deep thermal reservoir in conditions of equilibrium. The thermal springs with these hydrogeochemical characteristics differ in respect to the hydrochemical composition of the springs, formally described on several sites of BCS. Br/Cl and B/Cl ratios as well as the enrichment factor (EF) indicate that rainwater with a seawater component represents the source of the thermal spring water. In the springs, a mixture between thermal water and surface water is observed, combined with a relatively deep water circulation, allowing a calcium–sodium exchange, according to the host rock geochemistry. The higher temperatures found at some hot springs are related to the main trace of the San José del Cabo Fault.

Responsible editor: Philippe Garrigues

✉ Pablo Hernández-Morales
hdez.pablo@gmail.com

[1] Universidad Autónoma de Baja California Sur, Carretera al Sur Km 5.5, CP 23080 La Paz, B.C.S, Mexico

Keywords Thermal springs · Geothermometry · Hydrogeochemistry · Alkaline waters · San José del Cabo Fault (FSJC) · Los Cabos Block (BLC) · Gulf of California

Introduction

Baja California Sur (BCS) is a region with a semiarid–arid climate where water scarcity is limiting the development of socio-economic activities and human welfare so that water availability presents a challenge for sustaining the population with potable water. The annual rainfall in the state does not exceed 200 mm, and torrential rainfall during the hurricane season is the main factor for groundwater recharge (Díaz et al. 2008).

Due to its landforms and hydrogeological conditions, there are no large aquifers in the state of BCS and because of the proximity to the coast, the over-exploitation during decades has caused a seawater intrusion, provoking serious problems in several aquifers (Cardona et al. 2004; Prol-Ledesma et al. 2004; Wurl et al. 2009).

Mexico has currently geothermal power plants in use, for example, the geothermal field *Los Azufres* in Michoacan, *Los Humeros* in Puebla, and *Cerro Prieto* field in the north of Baja California state. The Baja California peninsula is characterized as an area with geothermal anomalies (González-Ruíz et al. 2015). The state of BCS has a geothermal power plant located near the volcano Las Tres Virgenes, known as Las Tres Virgenes (LTV) geothermal field (Maya-González and Gutiérrez-Negrín 2007; Portugal et al. 2000; Verma et al. 2006; Arango-Galván et al. 2015). Mexico is the fourth largest producer of geothermal energy in the world in 2016 with 1069 MW of operating capacity (Bertani 2016; GEA 2016).

In the southern part of the peninsula, several areas with hot springs have been described or mentioned, for example, near

Cabo San Lucas, El Sargento, Buenavista, and El Triunfo, which reach surface temperatures up to 45 °C (Torres-Rodríguez 2000; López-Sánchez et al. 2006; Wurl et al. 2009; Arango-Galván et al. 2015). In the case of the Santiago watershed, the hot springs have not been reported with respect to the hydrochemical composition and their genesis.

The aim of this study was to determine the hydrochemical composition of water in the hot springs, estimate the most likely reservoir temperature, and recognize the possible source of recharging at thermal springs in the watershed of Santiago, BCS.

Location

The Santiago watershed with exoreic drainage covers an area of approximatly 800 km^2 (Fig. 1) and is located in the southeast of BCS, Mexico at a distance of about 100 km SE to the city of La Paz, the capital of the state. The main access to the study area is via the transpeninsular highway 1 (La Paz–San José del Cabo); also, many dirt tracks connect the main towns and villages in the zone.

Geological and structural settings

Regional geology

The Baja California (BC) Peninsula has their genesis linked to the opening of the Gulf of California (Martín-Barajas 2000; Sedlock 2003; Frizzell 1984; Busch et al. 2011). The peninsula exhibits a heterogeneous geology; the oldest rocks come from the Triassic to the Jurassic period. The existence of a volcanic arc, caused by subduction, led the formation of ophiolite rocks that are located in the region of Magdalena Bay and Vizcaíno desert. The Cretaceous and Tertiary periods are represented by intrusive alkaline igneous rocks intrusionated by leucocratic and mesocratic dikes. Also, Tertiary volcanic rocks are outcropping in the middle of the Peninsula, sensu lato they are represented by volcanosedimentary rocks deposited alternating with lava flows at different stages in terrigenous and marine environments. Contemporaneously to the extension of the Gulf of California, tectonic basins were formed in marine and terrigenous environments. The latest geological deposits are represented by sediments in active streams, alluvial fans, terraces, dunes, and coastal sediments (Gastil et al. 1976; Hausback 1984; Sedlock et al. 1993; Martínez-Gutiérrez and Sethi

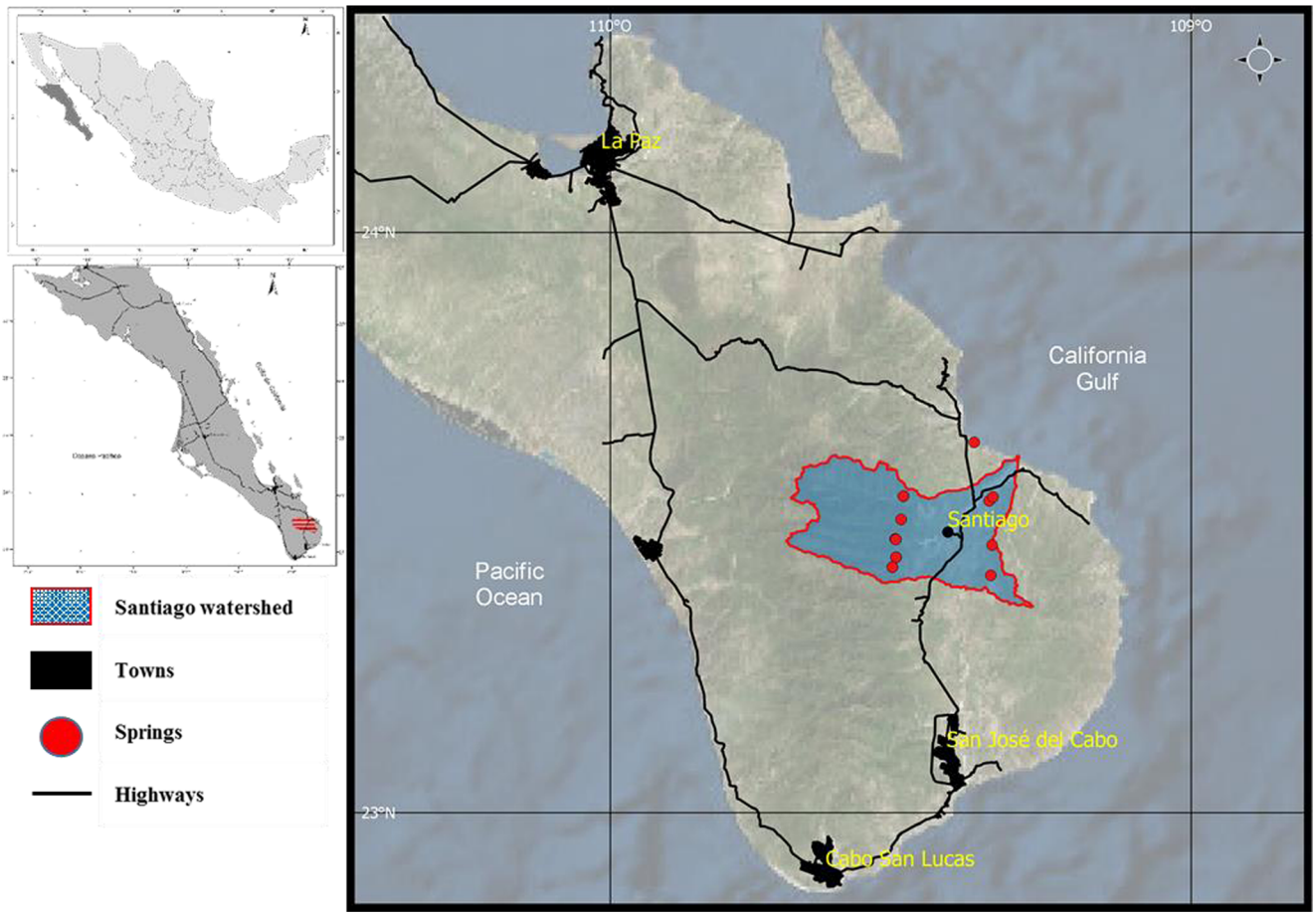

Fig. 1 The Santiago watershed, thermal springs, and main roads in the southern part of the Baja California peninsula

1997; Schaaf et al. 2000; Martín-Barajas, 2000; Kimbrough et al. 2001; Umhoefer et al. 2001; Dorsey et al. 2001; Busch et al. 2011).

Study area geology and previous works

Pantoja-Alor and Carrillo-Bravo (1966) and McCloy (1984) presented the first stratigraphic and lithologic descriptions of igneous and sedimentary rocks as well as some biostratigraphal datings in the area. Aranda-Gómez and Pérez-Venzor (1989) studied the metasediments on the west side of the Los Cabos Block (BLC), provide an age of 115-65 Ma for the metasediments and the pre to syntectonic plutons through K-Ar dating method. Additionally, deformed granites are found in the east and central part of BLC. Nevertheless, most of the rocks of the BLC are crystalline type corresponding to granitic to tonalitic composition, emplaced in the Mesozoic to Tertiary (Schaaf et al. 2000; Fletcher et al. 2003; Pérez-Venzor 2013). The Metamorphic complex represents the oldest rocks in the area and is formed by relicts, screens, roofpendants, apophisys, and dikes of metamorphic rocks with several degrees of ductile and/or brittle metamorphism and granitic rocks (Fig. 2) as well as the own granitic intrusives (sensu lato).

Martínez-Gutiérrez and Sethi (1997) describe the following five stratigraphic formations in the basin: La Calera, Trinidad, Refugio, Los Barriles, and El Chorro, which range from the middle Miocene to Pliocene (Busch et al. 2011; Martínez-Gutiérrez and Sethi 1997). The most recent deposits are found in the active streams as an alluvial sediments and on the slopes of the mountains as alluvial fans and alluvial terraces.

The BLC is considered a *horst* and the tectonic basin as a half *graben*, which was formed in association with the opening of the Gulf of California, giving rise to the extension of the basin San José del Cabo Basin (CSJC), during the Miocene–Pleistocene (Martínez-Gutiérrez and Sethi 1997).

Structural settings

The extensional province of the Gulf of California has been the subject of numerous studies (Stock and Hodges 1989; Lee et al. 1996; Martín-Barajas 2000; Fletcher and Munguía 2000; Umhoefer et al. 2002; Sutherland et al. 2012; Dorsey and Umhoefer 2012; Portillo-Pineda 2012). The predominant structural geologic features in BCS are of convergent Andean type, which started in the late Paleozoic and culminated in the late Cenozoic. The main pulses of magmatism occurred on the peninsula from about 120 to 90 Ma ago (Fletcher et al. 2003).

A convergent margin subduction regime evolved into an extensional margin, facilitating the development of a continental rift and then an oceanic rift. This process resulted to the transfer of the peninsula of Baja California to the Pacific plate during the late Miocene–Pliocene (Martín-Barajas 2000). Tectonic activity during and after the process of divergent oblique movement, influenced the formation of *grabens*, which were filled with sediments, as in the case of CSJC. The CSJC corresponds to a half *graben*, bounded by the San José del Cabo Fault (FSJC) normal listric type, with trend NNE–SSW (Martínez-Gutiérrez and Sethi 1997; Weber 2012). This fault is the main structure in the area. The fault also defines the contact between intrusive rocks and sedimentary rocks within the CSJC.

The FSJC is segmented and presents differential activity in each of its blocks, defined by the geometry of the mountain fore of each segment. The FSJC dissects and limits the oldest structures that are oriented with preferential direction between 10° and 15° to NW–SE (Fig. 2) (Martínez-Gutiérrez and Sethi 1997; Fletcher and Munguía 2000; Pérez-Venzor 2013). The BLC shows an intense fracturing, which defines a strongly steep topography. A fault known as La Trinidad fault limits the CSJC at the southeast border toward La Trinidad range (out of visible area in the geologic map). Both faults are defined as normal type (Martínez-Gutiérrez and Sethi 1997; Fletcher and Munguía 2000; Bravo-Pérez 2002). Faults in the Sierra La Trinidad mountain range show a north–northwest to northwest trend (Martínez-Gutiérrez and Sethi 1997). Tectonic activity began first in the Sierra La Trinidad (middle Miocene) and then in the BLC (late Pliocene) (Martínez-Gutiérrez and Sethi 1997), between 9 and 11 Ma (Fletcher et al. 2003).

Based on geophysical exploration, Busch et al. (2011) conclude that the listric normal movement of the FSJC was developed in stages, resulting in a differentiated architecture of sedimentary formations in the basin.

Hydrogeological gramework

The maximum altitude in the Santiago watershed reaches 2040 m a.s.l. at the east part of the study area. The mountain areas show a very precipitous relief with abrupt slopes, typically coming from granitic crystalline rocks (Martínez-Gutiérrez et al. 2010). In the elevated portions of the basin, the runoff flows with high velocity, generating vertically rather than horizontally erosion (Lugo-Hubp 1990). Therefore, the weathering caused by rain is the main factor that is modeling the basin. Erosive products, as cliffs and deep valleys were created, and blocks from meter size to fine particles, such as sand and silt, can be transported in the streams. The stream channels can measure up to kilometer wide, forming an unconfined and coastal aquifer (CONAGUA 2015).

In the central part of the watershed, tablelands composed with sediments of continental and marine origin with low dissection remained. The topography is dominated mostly by a dendritic and rectangular drainage pattern (Martínez-Gutiérrez et al. 2010). The Santiago watershed is draining to the eastern slope of BLC from the Sierra La Laguna toward the Gulf of California.

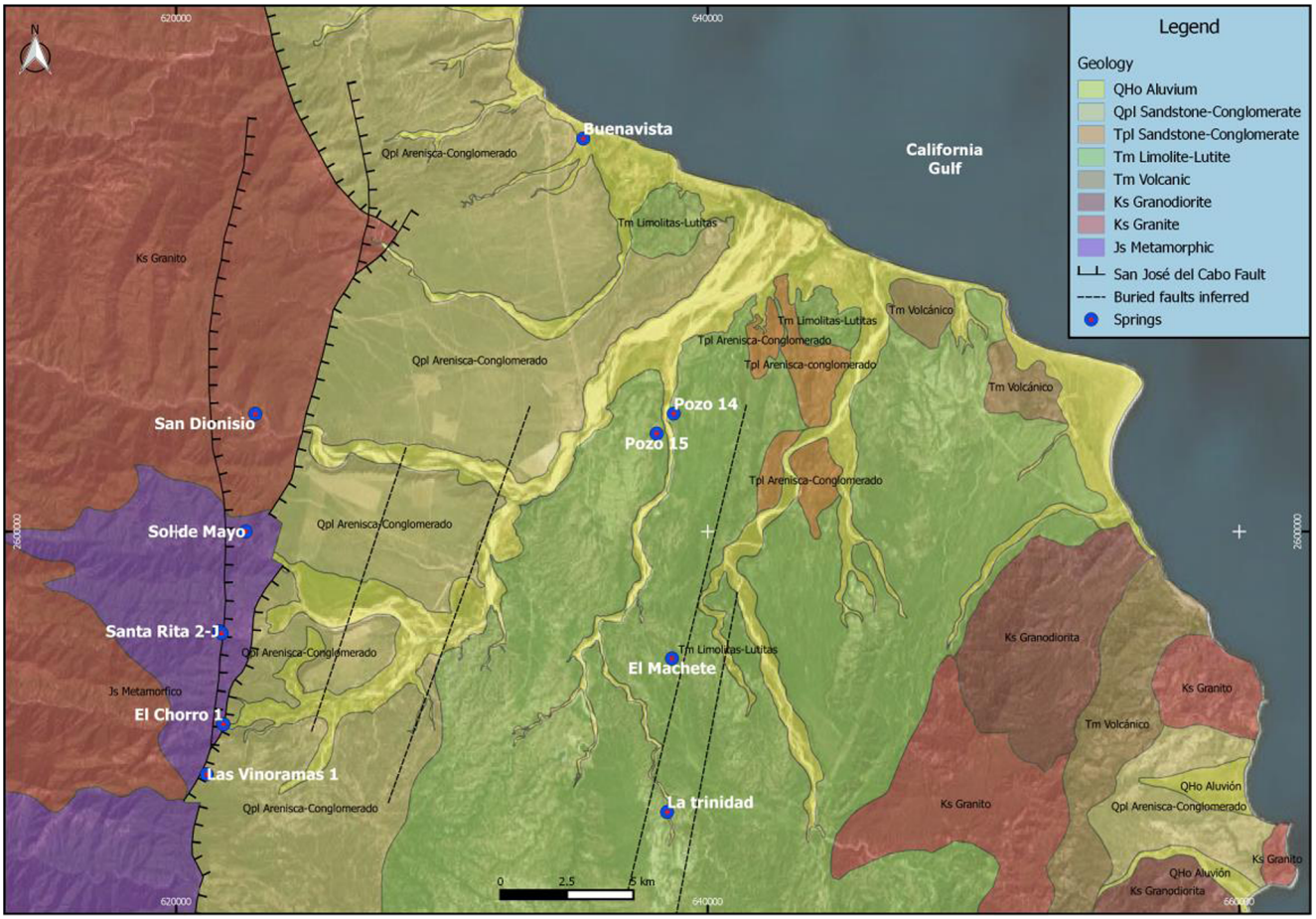

Fig. 2 Geological and structural maps showing geological and lithological units. Hot springs are located on the trace of San José del Cabo Fault and in the La Trinidad mountain range (modified after Martínez-Gutiérrez and Sethi 1997; Pérez-Venzor 2013; Inferred faults from Busch et al. 2011)

Geothermal and hydrogeochemical framework

Hydrogeochemical investigations have been conducted to determine the status of the aquifers. Because most of the population in BCS lives in the coastal zones, negative effects due to over-exploitation have been found, mainly due to the intrusion of seawater (Cardona et al. 2004; Prol-Ledesma et al. 2004; Wurl et al. 2009; Rosales-Ramírez et al. 2011; González-Abraham et al. 2012). Moreover, some negative effects also come from mining or industrial activity (Carrillo-Chávez et al. 2000; Wurl et al. 2014).

The presence of hydrothermal manifestations has been studied during the last 30 years. In order to recognize the geothermal potential in BCS, several researchers had developed knowledge through scientifics works, specifically for the Las Tres Virgenes geothermal field, where today, geothermal energy production plant in the municipality of Mulege exists. Also, other areas with geothermal activity exist, as in Loreto, Bahia Concepcion, Cabo San Lucas, San Juan de los Planes, and Santiago (Portugal et al. 2000; López-Sánchez et al. 2006; UABC 2011; Wurl et al. 2014; Tello-Hinojosa et al. 2005; Arango-Galván et al. 2015).

Torres-Rodríguez (2000) report a geothermal chart scale 1: 2,000,000 for Mexico, which includes the thermal zones existing on Santiago watershed and other places located in the Baja California peninsula.

Hydrothermal activity on the peninsula is linked to regional faults that allow deep penetration of water in areas of high heat flow (Prol-Ledesma et al. 2005). Faults are related to extensional tectonics of the Gulf of California in the Tertiary (Aranda-Gómez et al. 2000; Prol-Ledesma et al. 2004; Canet et al. 2005; Villanueva-Estrada et al. 2005).

So far, the work on hot springs on the peninsula indicates the seawater as a supply source, modified by geothermal processes. The thermal water is enriched in Ca, As, Hg, Mn, Ba, HCO_3, Li, Sr, B, I, Cs, Fe, and Si relative to seawater (Villanueva-Estrada et al. 2005).

Prol-Ledesma et al. (2005) describe similarities in the chemical composition of hydrothermal manifestations submarines in Punta Mita and Punta Banda. Villanueva-Estrada et al. (2005) proposed that water from springs in Bahia Concepcion is very similar to the composition of the thermal fluid found in deep wells of Las Tres Virgenes. Temperature calculated by

geothermometers reaches the deep reservoir approximately 200 °C for Bahia Concepcion and an equilibrium temperature at the surface of about 120 °C (Villanueva-Estrada et al. 2005).

López-Sánchez et al. (2006) describe samples of thermal water taken from boreholes which were perforated to a desalination plant project located near the city of Cabo San Lucas. They presented in their study the water type and origin of these sources, concluding that the reservoir has a temperature of 200 °C, with seawater as the dominant fluid and a chemical composition similar to that described for the central part of the Baja California Peninsula.

Wurl et al. (2009) conducted a study in which hydrogeochemical groups of groundwater were typified in the Santiago basin. They suggested that the eight water groups present a dominance of calcium-bicarbonate type. They indicate that some samples have a high salinity (greater than 1000 mg/L STD) and problems regarding the element nitrogen (in the ammonium and nitrite species), manganese, chloride, and chromium. According to the temperatures where water samples obtained (40 °C), the existence of thermalism in the zone was indicated.

González-Abraham et al. (2012) documented in his study geochemical samples of thermal springs in the region of Loreto and define the types of waters, determining the existence of mixtures of water and the ratio of the components in the water–rock interaction.

Arango-Galván et al. (2015) presented a compilation and characteristics of the main sites with geothermalism presence in the peninsula of Baja California. They propose 14 geothermal areas which include an area in the BLC near the town of Cabo San Lucas; however, they did not define hydrogeochemical characteristics for geothermal area in the Santiago watershed.

The Santiago watershed has low enthalpy geothermal resources (UABC 2011; Iglesias et al. 2011; Ordaz-Méndez et al. 2011). However, a detailed analysis of the characteristics of the thermal springs in Santiago has not been done.

Methods and data analysis

Sampling

A total of 16 water samples were taken at 9 springs, 1 handcraft well, and 1 well: eigth samples under dry conditions in June 2014 and eigth under humid conditions in March 2015, after the hurricane season of 2014, when hurricane Odile produced a maximum rainfall of 220 mm in the village of Santiago (Meteorological station Santiago 3062, CONAGUA 2014). The springs had low flow rate (less than 0.1 L/s), and one sample corresponds to an abandoned well with a diameter of 8″. Five springs were selected for repetitive sampling in the dry season and after heavy rain events: San Dionisio, Santa Rita 1, Santa Rita 2, El Chorro, and Las Vinoramas (Tables 1 and 2).

The sampling methodology and analysis methods were based on the Mexican standards: NMX-AA-003-1980 and NMX-AA-014-1980, the EPA/600/4-79-020 standard (US-EPA 1983), and the procedures defined in the Standard Methods for examinations of Water and Wastewater (SMWW 1999). The following informations were recorded: date and time; geographical position and altitude (with handle GPS Garmin®); the temperature was measured directly in the spring water with Hanna® termometer; electrical conductivity was measured with Hanna® conductivimeter; and the redox potential (in Eh mode) and pH were analyzed immediately after sampling with portable tester Hanna® Hi 98160.

The acidity and alkalinity were analyzed in the field by solution titration with 0.01 N HCl. The samples for cations and trace metals analysis were filtered through cellulose filters (0.45 μm of pore diameter) and then acidified with concentrated trace-metal grade HNO_3 (to reach pH ≤ 2) and stored at 4 °C. A second sample volume for the analysis of anions was taken, filtered in order to minimize bacterial activity. All the samples were collected in HDPE bottles previously washed with deionized water, and before taking the sample at the site the bottles were rinsed with water from the spring or well, respectively, after taking samples they were stored in ice boxes during the field trip.

Analysis methods

All analyses were conducted in the laboratories of the Institute of Geology/Faculty of Engineering of the Autonomous University of San Luis Potosi (UASLP). The major anions Cl, HCO_3, and CO_3 were analyzed by volumetric methods and SO_4, NO_3, and F by turbidimetric Spectrophotometer (Hach® model DR2800). The analysis of the cations Na and K was performed by flame spectrophotometer (Thermo Scientific® brand), and the elements Ca, Mg, B, and Si were obtained by inductively coupled plasma optical emission spectrometry (ICP-OES, Thermo Scientific® brand iCap 7000 model series). Trace elements were analyzed, using inductively coupled plasma mass spectrometry (ICP-MS, Thermo Scientific® Model X-series 2). The analytical data for ICP-OES and ICP-MS were verified calibrating the equipment with standards concentrations, blanks, and duplicates. Mean concentrations for samples analysis were obtained from three simultaneous measurements in both ICP equipments; the RSD was less than 2% (Table 3). The results of chemical analysis were validated based according to their charge balance, allowing only differences less than ±5%.

Table 1 Chemical analysis results (mg/L) and error in percent for samples in dry season

Sample ID	San Dionisio	Santa Rita 1	Santa Rita 2	El Machete	Pozo 15	Pozo 14	El Chorro	Las Vinoramas
X wgs84	622,977	621,711	621,628	638,659	638,082	638,725	621,782	621,149
Y wgs84	2,604,438	2,596,184	2,596,251	2,595,229	2,603,691	2,604,444	2,592,754	2,590,874
Alt. (m)	259	255	272	167	63	54	195	322
Temp (°C)	36.4	42.1	42.2	28.7	36.8	32.0	43.0	31.1
ORP (mV)	46.3	50	270	45	111	58.9	−300	10
pH	8.5	9.2	9.5	8.3	8.59	8	9.22	7.1
E.C (μS/cm)	616	299	240.6	546	730	2865	250	190.6
TDS	302	146	118	267	358	1404	123	93
Ca^{++}	13.52	8.68	4.16	21.84	13.89	31.25	8.68	6.94
Mg^{++}	11.38	1.06	0.63	2.53	1.06	2.11	1.06	2.11
Na^{+}	55.54	43.00	50.00	75.00	148.00	632.00	40.73	30.00
K^{+}	14.86	1.41	0.79	2.95	0.35	6.85	0.43	1.27
Cl^{-}	60.75	12.51	14.29	67.90	30.38	348.43	10.72	12.51
HCO_3^{-}	143.96	86.38	74.86	54.53	255.59	69.10	109.07	86.38
CO_3^{--}	5.66	11.33	16.99	10.73	21.15	5.66	0.00	0.00
SO_4^{--}	2.00	14.00	1.00	70.00	55.00	770.00	1.00	1.00
NO_3^{-}	1.50	0.80	0.80	5.00	0.60	1.70	0.70	0.80
F^{-}	0.58	2.29	2.13	0.22	1.54	1.29	0.48	2.27
% Error	0.56	−2.89	2.34	−0.84	1.69	3.75	3.49	−1.69

Data interpretation

The different types of water were classified, based on the concentration of major ions; Piper and Stiff diagrams were used to visualize the hydrogeochemical classification (Fig. 3).

Based on the enrichment factor (EF) the water source of the hydrothermal system can be recognized. For example, the concentration of an element, which is considered conservative, may indicate the evolution of seawater during elemental enrichment during evaporation (Vermette et al. 1988; Okay

Table 2 Chemical analysis results (mg/L) and error in percent for samples in wet season

Sample ID	La Trinidad	El Chorro 1	Las Vinoramas 1	Santa Rita 2-J	Santa Rita 1-J	Sol de Mayo	San Dionisio 1	Buenavista
X wgs84	638,475	621,782	621,149	621,628	621,711	622,613	622,977	635,322
Y wgs84	2,589,448	2,592,754	2,590,874	2,596,251	2,596,184	2,600,003	2,604,438	2,614,790
Alt. (m)	221	195	322	272	255	381	259	15
Temp (°C)	28.5	45.4	30.2	41.6	42.4	28	28.1	41.3
ORP (mV)	100	−304	−45.9	−427	−481	71	101.2	36.1
pH	7.17	9.44	9.07	9.22	9.11	8.05	8.9	8.04
E.C (μS/cm)	534	149	219.9	280	276.9	429	186.3	773
TDS	262	73	108	105	136	210	91	379
Ca^{++}	48.61	1.04	1.74	8.68	2.08	26.04	10.42	5.20
Mg^{++}	19.00	1.90	0.11	1.06	0.63	5.28	5.28	0.63
Na+	35.00	40.00	59.00	50.00	67.00	64.30	31.37	152.00
K^{+}	2.57	0.59	1.11	0.66	0.56	2.35	4.60	4.31
Cl^{-}	35.74	12.51	16.08	12.51	17.87	35.74	17.87	121.50
HCO_3^{-}	172.75	63.34	98.16	109.41	103.65	161.24	97.89	80.62
CO_3^{--}	0.00	11.33	10.73	11.33	11.33	0.00	5.66	11.33
SO_4^{--}	67.00	3.00	10.00	7.00	6.00	28.00	0.90	59.00
NO_3^{-}	1.90	0.60	0.70	0.70	1.20	0.70	0.70	7.20
F^{-}	0.18	1.84	2.55	1.91	4.57	0.35	0.20	2.22
% Error	2.82	0.64	−1.53	−1.26	1.97	3.71	2.07	3.27

Table 3 Chemical results for B, Br, and Si (mg/L)

Sample ID	B	Br	Si
San Dionisio	0.058	0.184	25.732
Santa Rita 1	0.121	0.037	20.924
Santa Rita 2	0.141	0.062	21.112
El Machete	0.150	0.343	20.200
Pozo 15	0.396	0.367	11.465
Pozo 14	1.207	2.855	11.311
El Chorro	0.131	0.061	16.150
Las Vinoramas	0.141	0.068	16.841
La Trinidad	0.118	0.204	16.446
El Chorro 1	0.131	0.060	16.283
Las Vinoramas 1	0.128	0.055	16.539
Santa Rita 2-J	0.167	0.079	21.470
Santa Rita 1-J	0.157	0.073	21.692
Sol de Mayo	0.123	0.260	24.073
San Dionisio 1	0.034	0.083	16.437
Buenavista	0.330	0.571	30.676
Seawater[a]	4.6	65	3
% RSD	1.67	1.37	1.84

[a] Seawater from Hill (2005)

et al. 2002). The method is feasible to recognize elements, incorporated into the water, by their enrichment regarding that source, applying the formula:

$$\mathrm{EF}_x = \frac{\left(\frac{x}{\mathrm{Cl}^-}\right)_s}{\left(\frac{x}{\mathrm{Cl}}\right)_{\mathrm{sw}}}$$

where the ratio x/Cl^- is the value for the sample and reference, respectively, in this case, seawater (sw). The value x is given for the concentration of the element to obtain in each sample.

The EF was used to define the water origin source for thermal springs. The diagram, proposed by Vengosh (2003), allows recognizing the salinity origin of the severals water sources (seawater, dissolution of evaporites, irrigation return flow from agriculture and hydrothermal water) through the ratios Br/Cl and B/Cl. It permits also to recognize effects caused by the evaporation of the source water (indicated with an arrow, see Fig. 6).

Calculations of different geothermometers (taking in account the concentration of SiO_2 and Na–K–Mg cations) allowed to estimate the equilibrium temperatures in the thermal reservoir. The data were processed within the software SolGeo (Verma et al. 2008) and in a spreadsheet designed by Powell and Cumming (2010). Several geothermometric equations are used in SolGeo and in the Powell and Cumming spreadsheet (i.e., Fournier 1979; Fournier and Potter 1982; Nieva and Nieva 1987; Giggenbach 1988; Verma and Santoyo 1997; Gunnarsson and Arnórsson 2000; Arnórsson 2000b; Díaz-González et al. 2008), given a useful tool to estimate temperatures at depth.

Results

Physicochemical analysis

The water samples, collected in the eastern part of the Los Cabos Block, presented the following hydrogeochemical characteristics (Fig. 3; Tables 1 and 2).

Weather conditions and temperature

The samples were taken under sunny weather conditions where the air temperature during the field campaign reached a maximum of 32–34 °C in June 2014 and 25–28 °C in March 2015. The average temperature in March was 18 °C and in June 27 °C, and the annual average is 22.8 °C, standard deviation 0.3 (Santiago weather station 3062, CLICOM 2015).

The highest water temperature corresponds to the thermal spring El Chorro with 45 °C, and the lowest temperature was observed at the spring Sol de Mayo with 28 °C (Fig. 3; Tables 1 and 2). The map (Fig. 3) and Tables 1 and 2 shows the water temperatures of the springs and the wells in the Santiago basin.

pH and Eh

The thermal springs have alkaline pH in the range of 8.5 to 9.5 (Santa Rita, El Chorro, Las Vinoramas, Buenavista), with exception of La Trinidad with value very closed to neutral pH. The lowest redox potential was observed at the spring El Chorro with −300 mV in June 2014 and −481 mV in March 2015 at Santa Rita 1 spring (see Tables 1 and 2). Eh values obtained indicate that the water in the springs of the Sierra La Laguna has an anoxic source at depth.

It is inferred that the processes of water–rock interaction allow rainwater to acquire a more alkaline pH during the migration in depth to interact with mineral alteration product (Feldspar mainly), which is involved in ionic reactions in the water–rock interaction, resulting in the change of an acidic-neutral pH (rainwater) to a more alkaline.

Electrical conductivity

The average electrical conductivity was 261 μS/cm; the lowest value corresponds to the El Chorro 1 spring (after rainy season) and the highest to Pozo 14 (Tables 1 and 2). The Pozo 14 is located inside an agricultural field, so the elevated mineralization may be caused by the recirculation due to irrigation of water which infiltrates in the crop field.

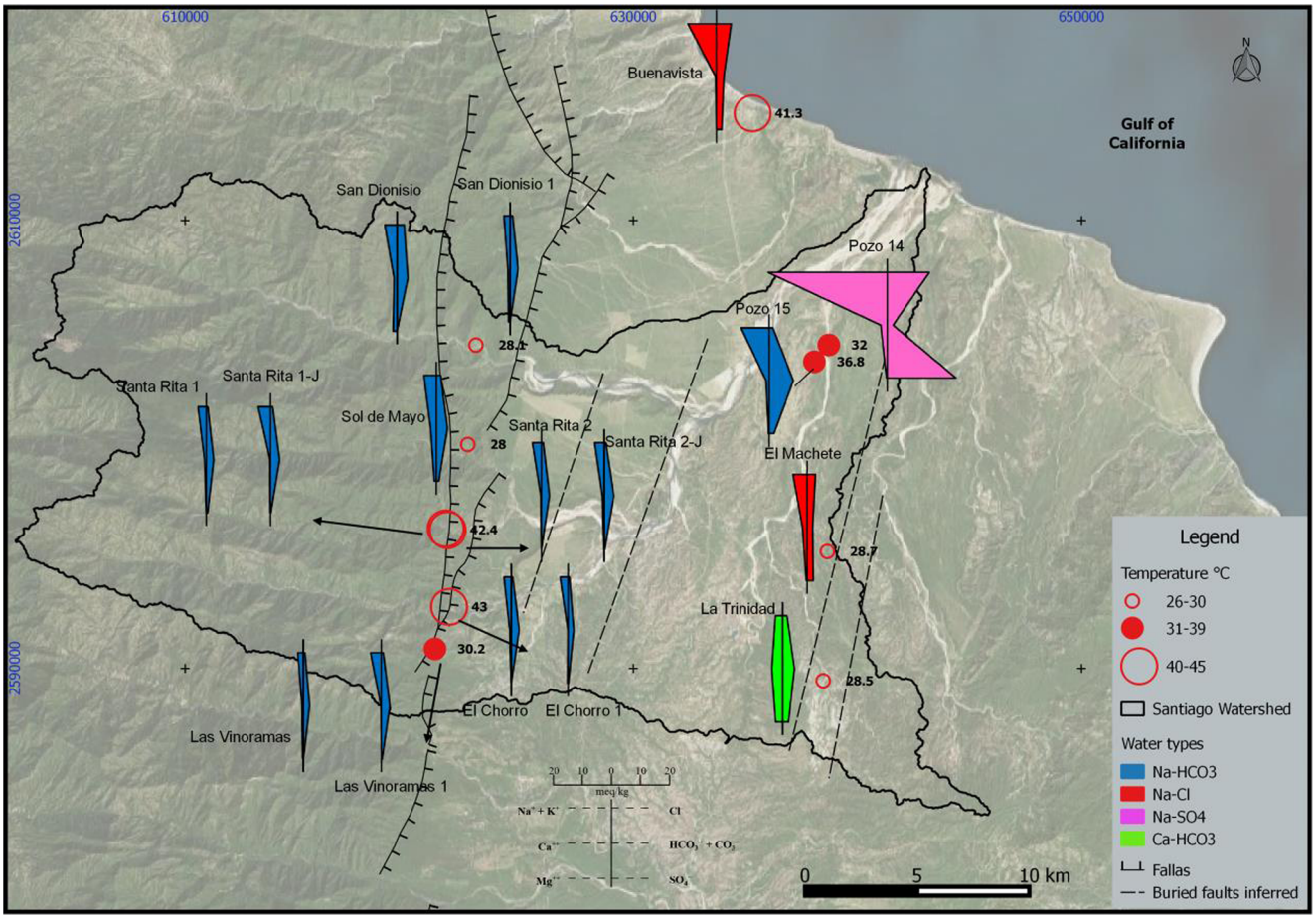

Fig. 3 Hydrogeochemical map with the characterization of the thermal springs (Stiff diagrams) and temperature

The low mineralization in water at the springs suggests a relatively fast migration in depth, which may be due to high hydraulic conductivity product of the intense fracturing. A steam–water phase may be causing dilution during the water ascent. Mineral precipitation by conductive heat loss and mixing with meteoric water is possible, so this could be a reason for the low mineralization observed. The Buenavista sample showed 773 μS/cm; it is located near the coast and may be affected by mixing with seawater (Fig. 3).

Thermal springs water clasification

The samples were classified with respect to their abundance of major ions. El Chorro, Las Vinoramas, Santa Rita, Sol de Mayo, San Dionisio, and Pozo 15 predominate the sodium bicarbonate type. Buenavista and El Machete correspond to the sodium chloride type; meanwhile, La Trinidad belongs to the calcium-bicarbonate type and Pozo 14 resulting sulfate sodium type (Figs. 3 and 4).

All 16 samples are presented in the Piper (1944) diagram (Fig. 4). The diagram allows to recognize mixing processes between the different types of water. One mixing line is visible between thermal water and more (San Dionisio 1) or less meteoric water (Las Vinoramas and Santa Rita 1). A second mixing line can be identified between San Dionisio 1 and seawater, where El Machete is identified as most influenced by seawater mixing. It can also be observed that samples, taken after the rainy season, show a relative increase in the concentration of Na (San Dionisio 1, The Vinoramas 1, El Chorro 1, and Santa Rita 2) (Fig. 4).

Five samples, taken in the dry season, were compared to those obtained after the rainy season and low changes in their composition was observed (see Piper and Stiff diagrams; Figs. 3 and 4). In the dry season, a trend to acquire more calcium is observed.

The spring water in the Sierra La Laguna mountains (of sodium bicarbonate type) can be associated with a rapid flow of meteoric water into deeper zones and a subsequent return to the surface. El Chorro, Santa Rita 1, and Santa Rita 2 had higher pH values (up to 9.5) and higher temperatures than the northern springs (Sol de Mayo, San Dionisio; Fig. 3). Water samples from the eastern part of the basin (Pozo 14 and Pozo 15, La Trinidad, El Machete) show a generally higher mineralization probably due to the porous media formed by fluvial and marine sedimentary rocks.

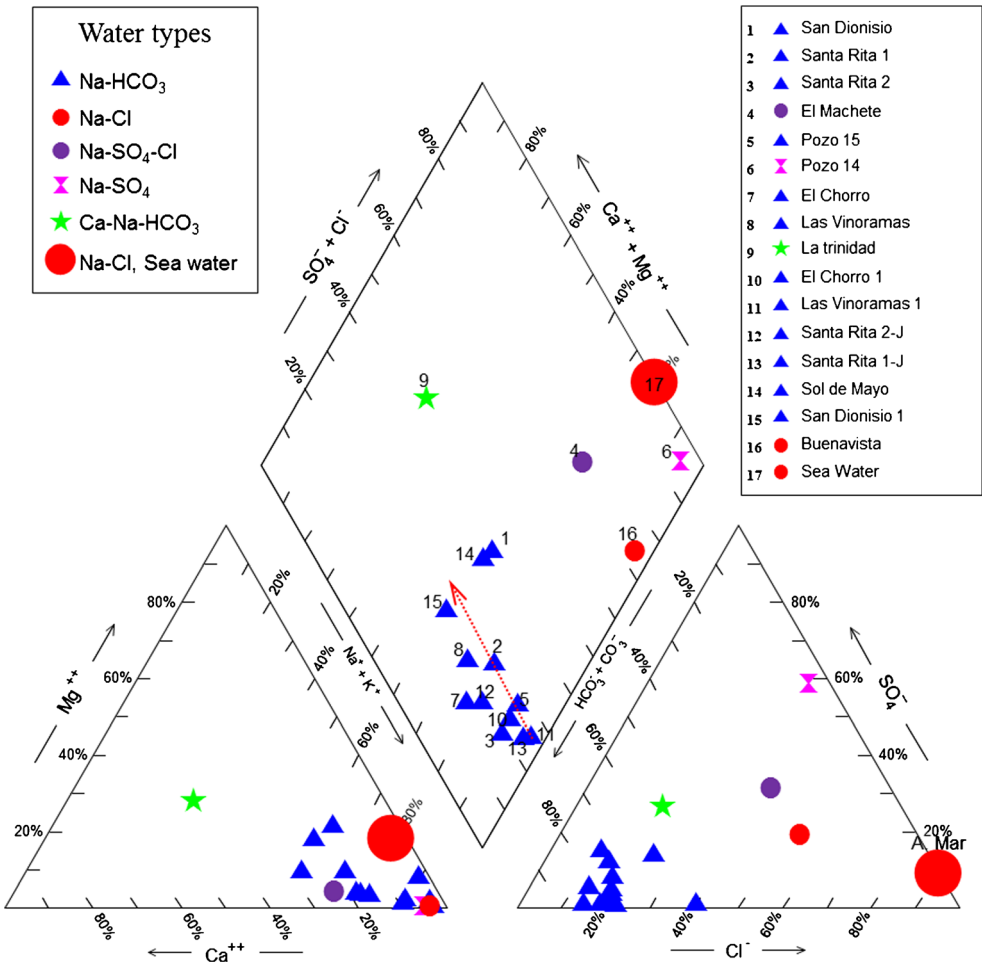

Fig. 4 Piper diagram with the hydrogeochemical signature of 16 samples. Seawater was included as reference (after Hill 2005). The maximum TDS concentration is 1404 mg/L (Pozo 14)

Br/Cl and B/Cl ratios

The ratios of Br/Cl and B/Cl were used in order to recognize the effects of evaporation, mixing, and the possible origin of the spring water; Cl, Br, and B are conservative elements (Arnórsson 2000a; Bear et al. 2013; Vengosh 2003). In the graph Br vs Cl (Fig. 5; Table 3), the spring water maintains the relation between this two elements, found in seawater.

Based on the diagram proposed by Vengosh (2003), the ratio of Br/Cl vs B/Cl allows to distinguish between different salinity sources in the springs and effects due to evaporation, so the relations mentioned would indicate water from different recharging provenances (Fig. 6).

The B/Cl ratios, measured in all the hydrothermal waters, differ in respect to the hydrothermal water with seawater as a source, described by Prol-Ledesma et al. (2004), Canet et al. (2005), and Villanueva-Estrada et al. (2005), among others. In the hydrothermal manifestations from the BLC, two different groups can be distinguished (red and purple in Figs. 5 and 6). The Br/Cl ratios varies between samples that coincide with the ratio in seawater and others where an evaporating process is indicated.

The diagram Br/Cl vs B/Cl shows samples within the area that define geothermal waters origin, and two groups are observed in the graph (Figs. 5 and 6). The most thermal group has a higher ratio B/Cl, allowing to recognize the possible addition of boron geogenic (Table 4). It is probable that the thermal spring areas in Las Vinoramas, El Chorro, Santa Rita 1, and Santa Rita 2 have their chemical composition influenced by water–rock interaction effects in the alteration zone generated by the San Jose Cabo fault (Fig. 3). Furthermore, the two clear trends of separate groups give an idea of mixing waters; samples with less B/Cl ratio would be defining mixing zones compared to those with greater B/Cl ratio. For two groups, it is observed that they have a certain linear relationship toward increased relations Br/Cl and B/Cl; this suggests a dilution probably caused by evaporation.

Enrichment factor

Based on the concept of conservative properties of some elements (i.e., Cl, B, Li), they can be used as a reference to define a possible enrichment for a given chemical element. Applying the EF formula, if the result is a value that tends to 1 in the

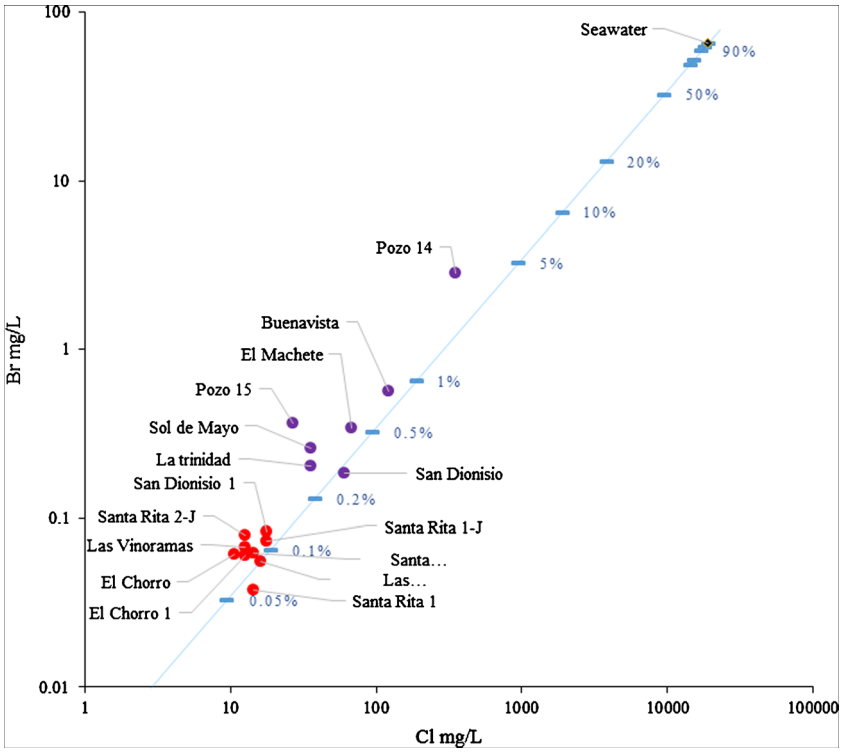

Fig. 5 The diagrams show the Br and Cl relation for the samples analyzed in the Santiago basin and reference seawater (Hill 2005). *Line* indicates the % dilution trend of the seawater. Additionally, two groups are observed in the diagram, one between 0.05 and 0.1% and the other at 0.2 and 1% *red* and *purple points*, respectively

reference–sample relationship, this indicates that the contribution comes from the used reference. A greater EF than 1 indicates an external enrichment in respect to the reference source (Vermette et al. 1988; Okay et al. 2002). This method is widely used to recognize sources, for example, rainwater. Usually, the method is used with the sodium in seawater and aluminum

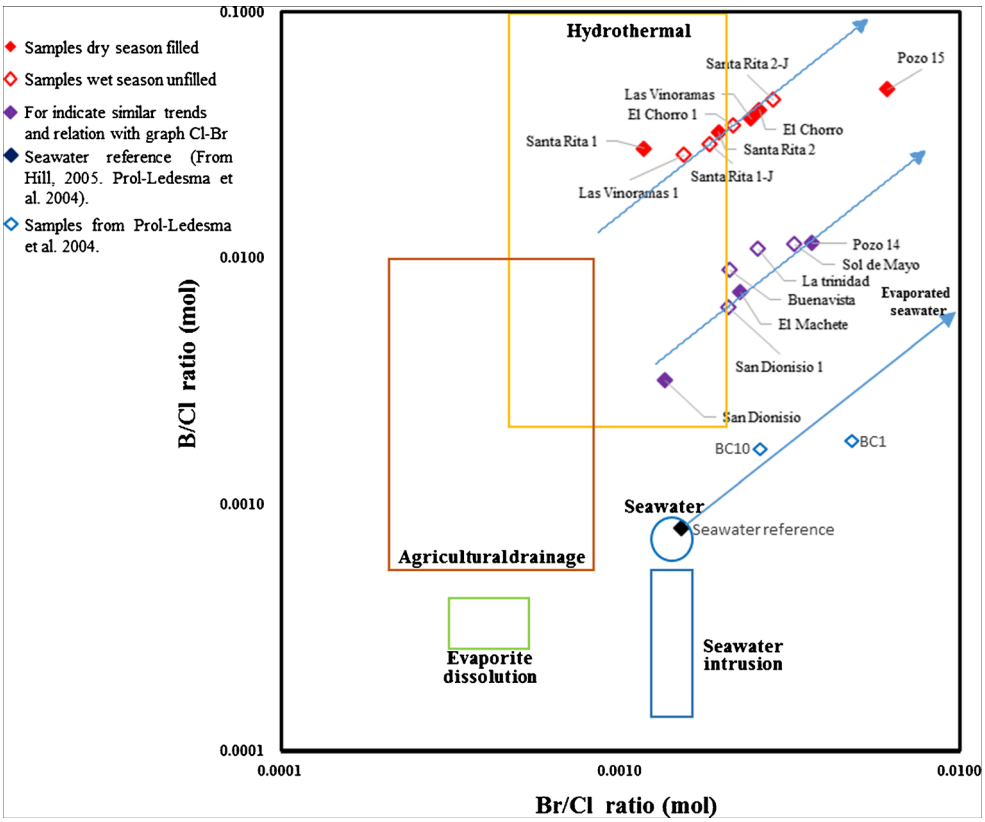

Fig. 6 Source of origin of water in samples according to the ratios Br/Cl and B/Cl (diagram after Vengosh 2003). *Arrows* indicate dilution by evaporation. Bromide vs chloride ratio (with respect to mol/L) of thermal waters from the study area (*filled points* indicate samples taken during the dry season) and samples reported by Hill (2005) and Prol-Ledesma et al. (2004)

Table 4 Enrichment factors to 16 samples in Santiago watershed

EF seawater	EF Na	EF Mg	EF F	EF B	EF Br	EF Si
San Dionisio	1.65	2.64	139.53	3.98	0.89	2682.56
Santa Rita 1	6.22	1.19	2675.86	39.96	0.87	10,595.01
Santa Rita 2	6.33	0.62	2177.79	40.74	1.27	9353.98
El Machete	2.00	0.52	47.35	9.09	1.47	1884.11
Pozo 15	8.82	0.49	740.97	53.85	3.53	2390.51
Pozo 14	3.28	0.09	54.11	14.31	2.39	205.60
El Chorro	6.87	1.39	654.36	50.35	1.67	9540.57
Las Vinoramas	4.34	2.37	2652.49	46.46	1.58	8527.43
La Trinidad	1.77	7.48	73.62	13.63	1.67	2914.64
El Chorro 1	5.79	2.13	2150.04	43.09	1.41	8244.78
Las Vinoramas 1	6.64	0.09	2317.52	32.82	1.00	6513.42
Santa Rita 2-J	7.23	1.19	2231.83	55.08	1.85	10,871.41
Santa Rita 1-J	6.79	0.50	3738.03	36.38	1.20	7688.69
Sol de Mayo	3.26	2.08	143.14	14.17	2.13	4266.29
San Dionisio 1	3.18	4.16	163.59	7.86	1.36	5826.00
Buenavista	2.26	0.07	267.04	11.20	1.37	1598.97

for the crust as reference. This paper used the Cl in seawater as reference instead of Na.

In respect to Cl in seawater, the EF for Na, Mg, F, Si, Br, and B was calculated. The results can help to elucidate if the recharge water of the springs has contribution and is diluted from seawater or, on the other hand, if it has other enrichment supply sources. Table 4 shows the EF calculated.

An EF between 1 and 10 indicates a considerable content of elements from the source (Vermette et al. 1988; Okay et al. 2002). F, B, and Si have high enrichment factors, because this elements are spiked due to disolution of minerals containing this elements, such as fluorite, quartz, feldspar, and alteration minerals. Especially, Br values are very close to 1 in all samples indicating their origin from the seawater. The silica and fluorine show very high values in the enrichment factor; its origin is attributed to the dissolution of minerals from the alteration in the fault zone of the granitic and metamorphic rocks of the BLC.

Geothermometry

Thermal water classification

Generally, it is necesary to define first which determinated type of geothermometer can be applied according to the chemical characteristic of the thermal water. Some diagrams can be used: The diagram proposed by Giggenbach and Goguel (1989) shows that there exists the dilution and mixing for the thermal water with the recharge surficial water that promove the low equilibrium in the thermal springs. The tendencial curve that the samples show toward the zone of

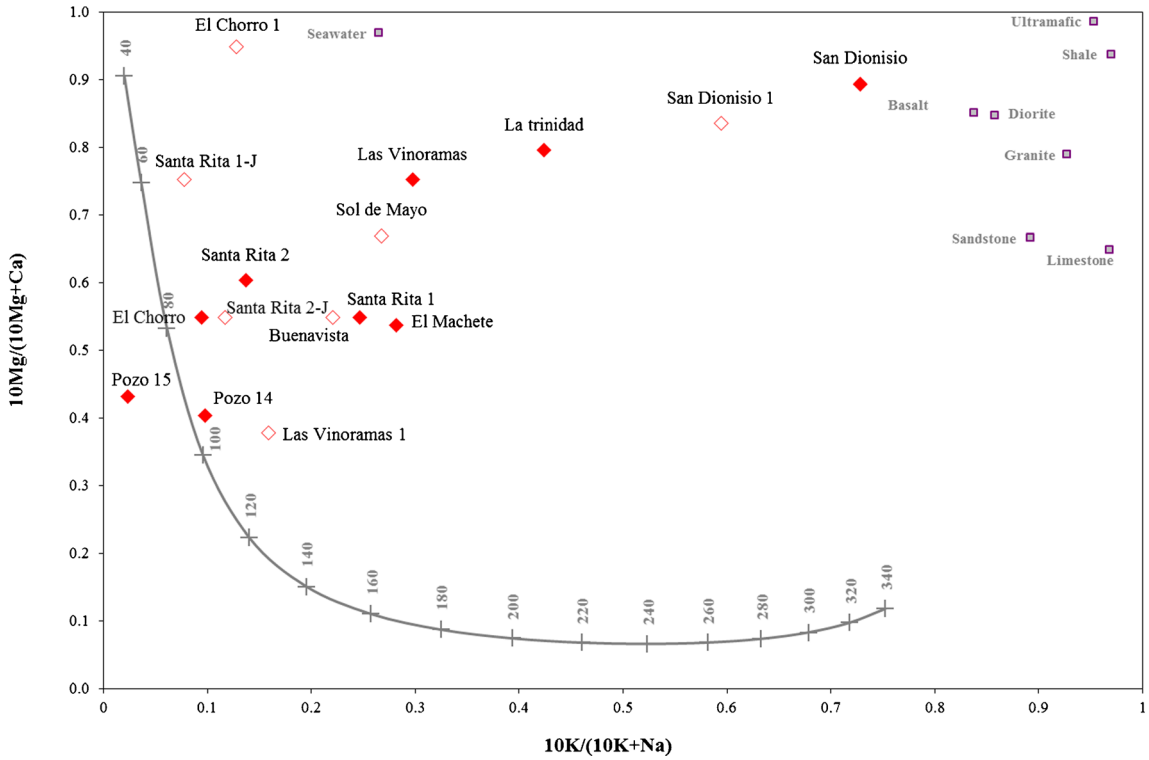

Fig. 7 The diagram after Giggenbach and Goguel (1989) shows the relation between Mg/(Mg + Ca) and K/(K + Na). The *curved line* indicates water rock equilibrium at different temperatures. Most of the samples studied are not in equilibrium, possibly due to mixing with rainwater. Samples with *filled marks* were taken during rainy season

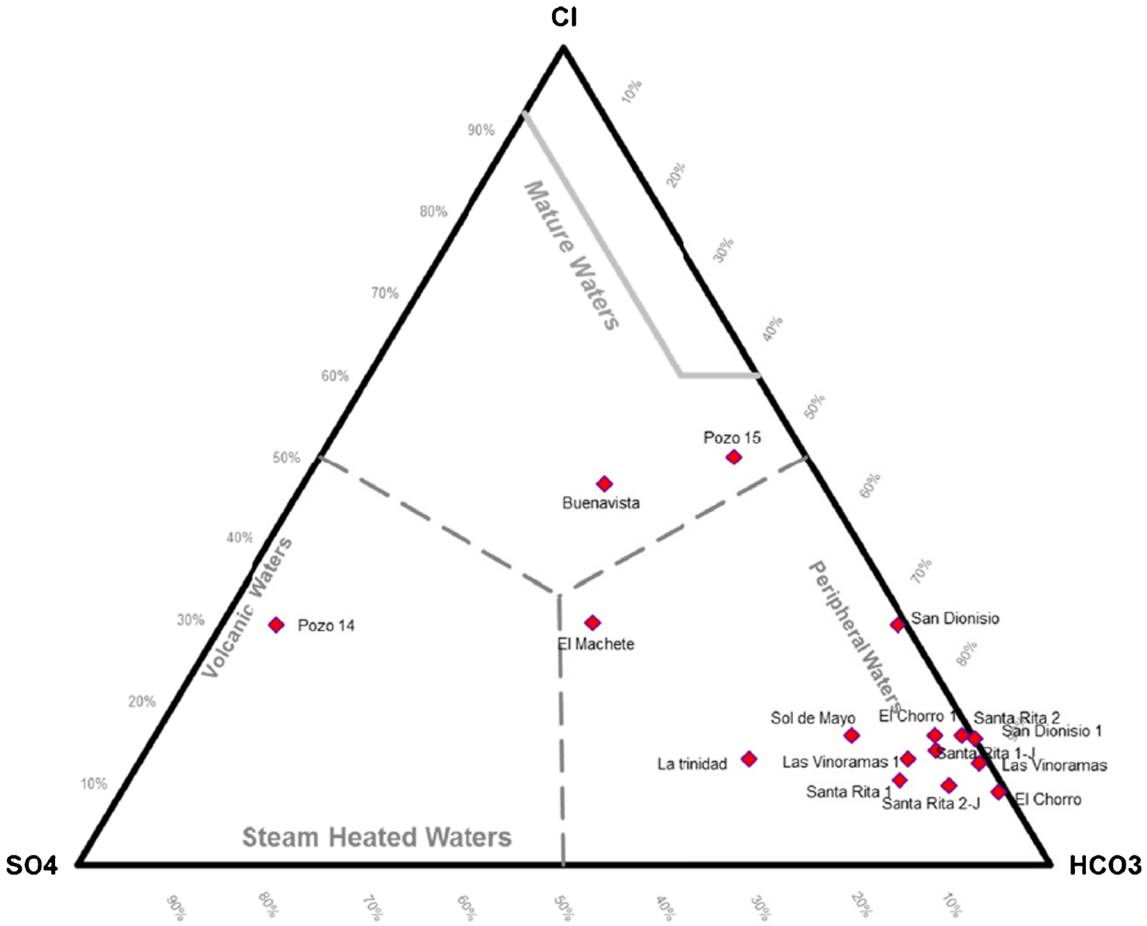

Fig. 8 Giggenbach ternary diagram of Cl, SO_4, and HCO_3 shows the classification of the majority of samples in the field of HCO_3, which could be explained as a mixing of thermal waters with surface waters

the rock dissolution is notable toward the equilibrium water rock line (Fig. 7).

The diagrams in Figs. 8 and 9 present the ion ratios of Cl–SO_4–HCO_3 and Cl–B–Li that allow to explain a probable mixture between water of the geothermal system with water at shallower meteoric water. The Cl–SO_4–HCO_3 diagram (Fig. 8) is used to distinguish the classification of thermal water basis in their principal anions; the majority of samples lie on the peripheral waters field (HCO_3) in the diagram and can be explained as thermal water influenced with surface waters enrichment in this anion. Cl–B–Li diagram (Fig. 9) indicates that the samples are in the zone with low absorption of Cl/B steam and represents an older hydrothermal system, indicating that the fluids had influenced by water rock interaction. The Na–K–Mg diagram (Fig. 10) shows that most of the samples are unreliable to estimate temperatures in their reservoir with cation exchange geothermometers; only the samples in the field of partial equilibrium of the reservoir temperatures could be estimated using these geothermometers but with rigorous caution.

The results obtained by the geothermometer silica and Na–K are shown below. Table 5 presents the results for several geothermometers calculated within the software SolGeo (Verma et al. 2008). This computer program allows the calculation to 35 geothermometric equations (for details of the statistical basis, see SolGeo; Verma et al. 2008). Some silica and cationic geothermometric formulas used were the proposed by Fournier and Potter (1982), Arnórsson (2000b), Giggenbach (1988), Nieva and Nieva (1987), and Díaz-González et al. (2008), among others.

Silica geothermometer

The temperature in the thermal reservoir for the samples taken at thermal springs, Las Vinoramas, El Chorro, Santa Rita 1, Santa Rita 2, Sol de Mayo, San Dionisio, and Buenavista, calculated for quartz geothermometer (Verma and Santoyo 1997), lay between 86 and 115 °C; the highest temperature for the deep reservoir corresponds to the spring Buenavista, although the highest surface temperature was observed at the El Chorro spring (45 °C).

Calculations for quartz geothermometer, using equations within SolGeo, for Fournier (1977) and Verma and Santoyo (1997), are similar. These geothermometers are valid for

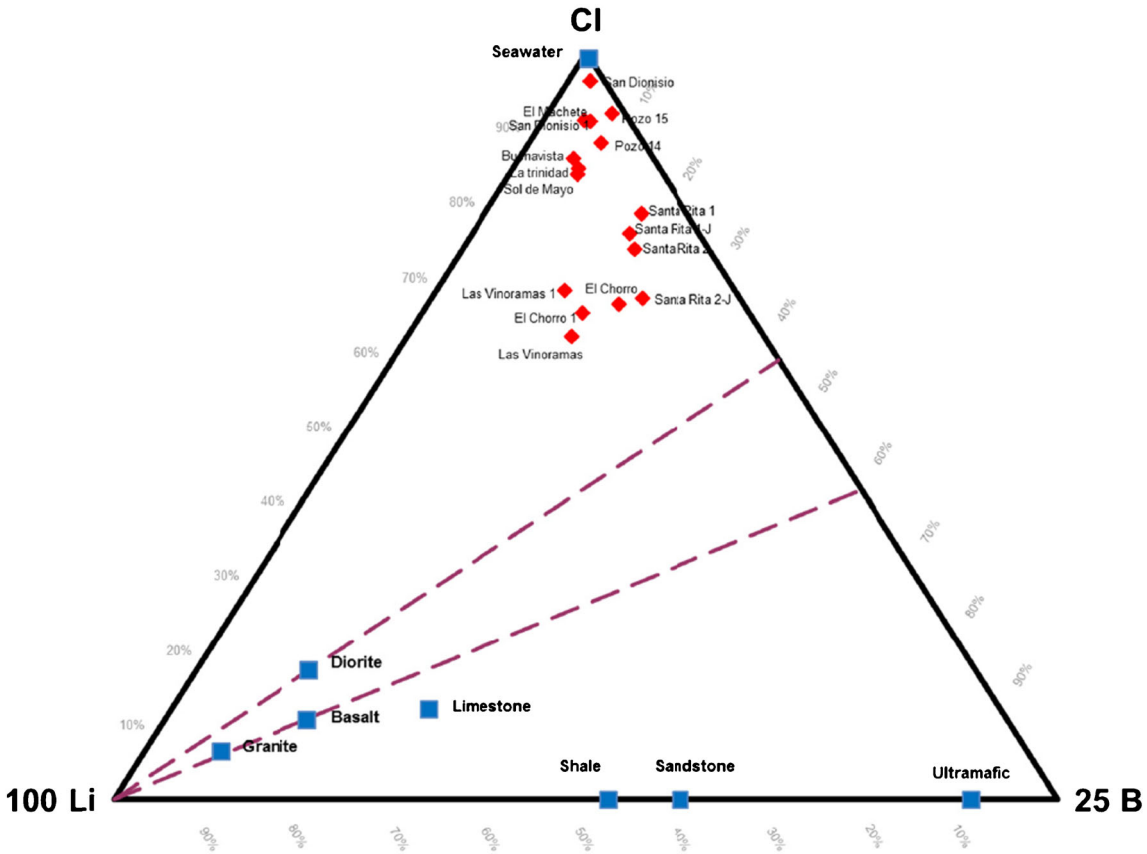

Fig. 9 Li–B–Cl diagram defines two groups of water. Major concentration in Li and B is typical for geothermal systems with fractionation associated to fluid heated by low temperature steam (Powell and Cumming 2010). The same separation in two groups is observed, as in the Br/Cl–B/Cl diagram (Fig. 6)

temperatures between 0 to 250 and 20 to 210 °C, respectively (Verma et al. 2008) and have the best representation to estimate the reservoir temperature of the thermal springs at the Santigo watershed. The minimum temperature was found for Pozo 14 with 71.5 °C and a maximum of 115.4 °C for the Buenavista spring. The samples show that the Si is in equilibrium with chalcedony (Fig. 11).

Exchange cationic geothermometer

The samples from the springs Las Vinoramas 1, Santa Rita 1-J, Pozo 15, Pozo 14, and Buenavista show a partial equilibrium in the Na–K–Mg diagram, pointing to a temperatures between 34 to 88 °C with the Na–K geothermometer by Díaz-González et al. (2008), 85 to 134 °C with Verma and Santoyo (1997) Na–K geothermometer, and 90 to 148 °C with the Giggenbach (1988) Na–K geothermometer (Tabla 5, the table presents the errors for Verma and Santoyo geothermometer and Diaz-González et al. geothermometer). The modeling with cations geothermometer presents problems to define with certainty an equilibrium temperature, and some authors suggest not to use the concentrations in these calculations, but the activity coefficients; others propose not to use them anymore because it is contrary to the laws of chemistry and thermodynamics (Arnórsson 2000b; Verma 2015).

Discussion

The springs in the BLC are embedded in crystalline and metamorphic rocks and are influenced mainly by the active fault of the San Jose del Cabo and differ in respect to the formally described springs in the north and middle of the Baja California peninsula, which correspond to activity volcanic system of Las Tres Virgenes (Portugal et al. 2000; Prol-Ledesma et al. 2004; Verma et al. 2006). Other springs in Loreto and Bahia Concepcion have manifestation in shallow submarines media (Prol-Ledesma et al. 2004; González-Abraham et al. 2012; Arango-Galván et al. 2015).

Temperatures up to 72 °C are reported in sodium chloride type water which are very similar to the chemical composition of the Buenavista spring but are noticeably different to the others analyzed sites in this study (Tables 1 and 2). For the Santiago watershed thermal springs, the maximum temperature observed in the field was only 45 °C.

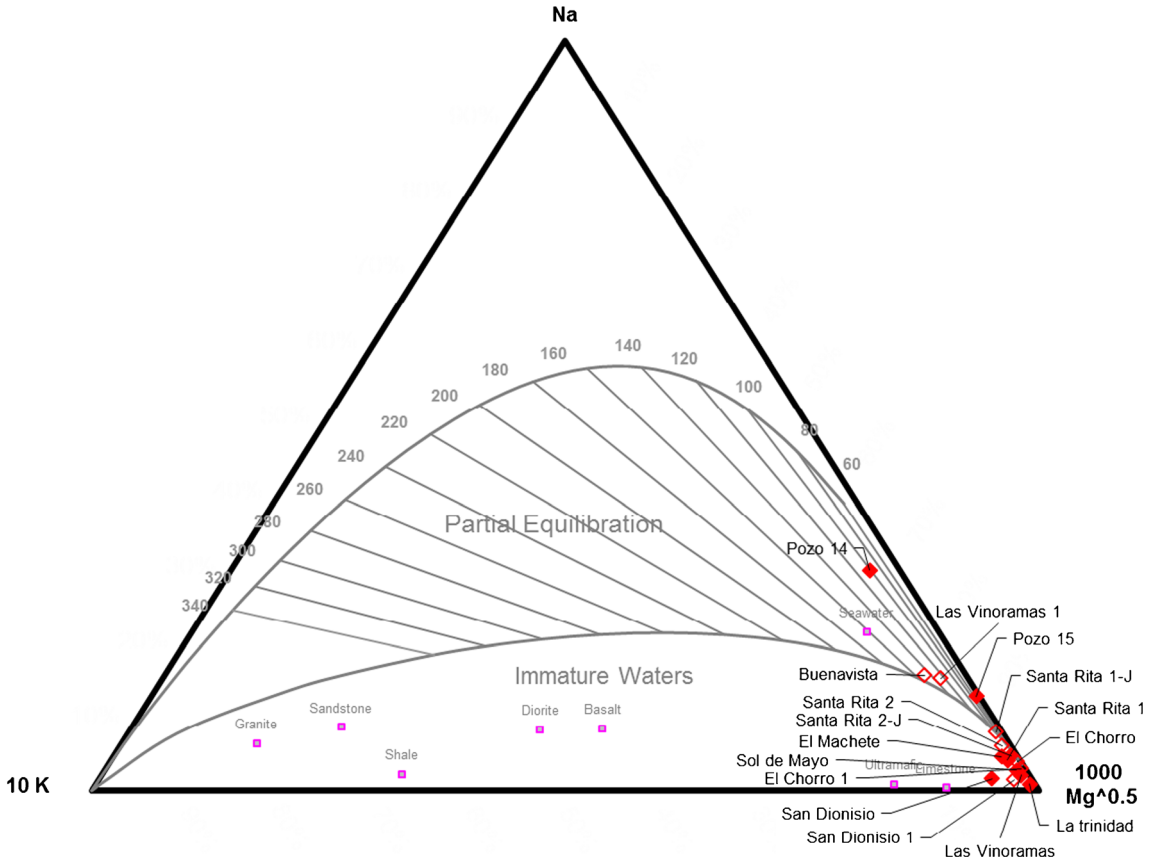

Fig. 10 Na–K–Mg diagram (Giggenbach 1988). Most samples lay in the field of inmature waters; however, Buenavista, Las Vinoramas 1, Santa Rita 1-J, Pozo 14, and Pozo 15 show partial equilibration, which permits to estimate their reservoir temperatures with cation geothermometers

Ramírez-Guzmán et al. (2004) indicate that a significant source of alkalinity, which would explain the increase of pH values in granitic rocks, represents closed system for CO_2 and low carbon carbonate concentration as well as a high proportion of water–rock interaction, favoring the dilution and depletion, and inhibits precipitation of secondary minerals. In the particular sense of geological and structural environment, thermal springs with similar characteristics exist in the state of Guerrero and Nayarit (Taran et al. 2013). The crystalline rocks of the BLC can be compared to the crystalline batholiths near Puerto Vallarta. Schaaf et al. (2000) found geochemical and isotopic similarities between the Puerto Vallarta batholith and Los Cabos Batholith.

The hydrogeochemical signature of the hot springs indicates the existence of Ca–Na ion exchange. It is understood that during the dry period, the system acquires hydrothermal fluid characteristics closer to the equilibrium. The Ca concentration decreased in samples from springs Santa Rita, El Chorro, Las Vinoramas, Sol de Mayo, and San Dionisio for the period after rain. During the dry period, the hydrothermal system would favor the increase of calcium, and in the rainy season, the mixture with meteoric water could cause more enrichment in sodium. Under the arid conditions of BCS, rains generally occur as a result of hurricanes. Therefore, the concentration of Na would be closely related to the chemical composition of rainwater, with a certain portion of seawater. Moreover, significant concentrations of Na and Ca have origin from the mineralogical composition of the rocks. The feldspathic minerals are characteristic for intrusive existing in the BLC (Schaaf et al. 2000) so that alteration of these minerals allows mobility effect in the concentrations of Na–Ca in spring water.

The EF obtained gives an idea of the quality of water that recharges the hydrothermal system. Especially in the hurricane season (May to November), rainwater could acquire the seawater signature, transferred by evaporation and incorporation of aerosols, as well as seawater in suspension, produced by large-scale weather systems (hurricanes up to category 4) that affect the area. Therefore, although the source of the water is presumably seawater, based on the results found by the EF, the acquirement of the marine signature is possible based on meteoric processes and not caused from a direct intrusion of seawater into the thermal system. The B/Cl and Br/Cl diagrams may as well support this and allow to separate two distinct groups, showing an evolution toward an enrichment in the ion ratios by evaporation (Fig. 6).

The calculated temperature, which resulted from chemical modeling through geothermometers, indicates that the heat

Table 5 Calculation of temperature in degrees Celsius, for several geothermometers, using SolGeo (Verma et al. 2008)

Sample ID	Na–K (Giggenbach 1988) TNKG88[a]	Na–K (Verma and Santoyo 1997) TNKVS97[a]	Error (Verma and Santoyo 1997) ENKVS97[a]	Na–K (Arnórsson, 2000b) TNKA00[a]	Na–K (Díaz-González et al. 2008) ec1 TNKDSR08[a]	Error (Díaz-González et al. 2008) ENKDSR08[a]	SiO_2 (Fournier 1977) ec1 TSF77[a]	SiO_2 (Fournier and Potter 1982) TSFP82[a]	Error (Fournier and Potter 1982) ESFP82[a]	SiO_2 (Verma and Santoyo 1997) ec1 TSVS97[a]	Error (Verma and Santoyo 1997) ec1 ESVS97[a]	SiO_2 (Arnórsson 2000b) TS2A00[a]
San Dionisio	325.3	316.1	59.5	313.0	328.9	17.4	106.4	106.8	3.5	106.9	2.5	92.8
Santa Rita 1	156.5	142.6	34.4	123.9	98.0	8.3	96.8	97.3	3.5	97.5	2.7	82.9
Santa Rita 2	118.5	104.4	29.8	88.9	54.7	7.0	97.2	97.7	3.5	97.9	2.7	83.3
El Machete	167.3	153.6	35.7	134.2	110.8	8.7	95.2	95.7	3.6	95.9	2.7	81.2
Pozo 15	44.5	30.7	22.1	22.0	–	4.9	71.4	71.8	4.0	72.0	3.5	56.8
Pozo 14	101.0	86.9	27.9	73.2	35.7	6.4	70.8	71.2	4.1	71.5	3.6	56.2
El Chorro	99.4	85.3	27.7	71.7	34.0	6.4	85.4	85.9	3.7	86.2	3.0	71.2
Las Vinoramas	171.9	158.2	36.3	138.7	116.3	8.9	87.2	87.7	3.6	88.0	2.9	73.0
La trinidad	208.9	195.9	41.3	176.2	162.4	10.4	86.2	86.7	3.6	87.0	2.9	72.0
El Chorro 1	114.8	100.7	29.4	85.6	50.7	6.8	85.8	86.3	3.7	86.6	2.9	71.6
Las Vinoramas 1	127.0	112.9	30.8	96.6	64.2	7.2	86.4	86.9	3.6	87.2	2.9	72.2
Santa Rita 2-J	109.8	95.7	28.8	81.2	45.2	6.7	98.0	98.4	3.5	98.6	2.7	84.1
Santa Rita 1-J	90.2	76.1	26.7	63.5	–	6.1	98.4	98.9	3.5	99.1	2.7	84.6
Sol de Mayo	163.0	149.2	35.2	130.1	105.7	8.5	103.3	103.7	3.5	103.8	2.6	89.6
San Dionisio 1	264.9	253.3	49.5	238.8	238.0	13.4	86.2	86.7	3.6	87.0	2.9	72.0
Buenavista	148.4	134.5	33.4	116.3	88.6	8.0	115.0	115.3	3.6	115.4	2.5	101.7

[a] Geothermometers codes are from Verma et al. 2008

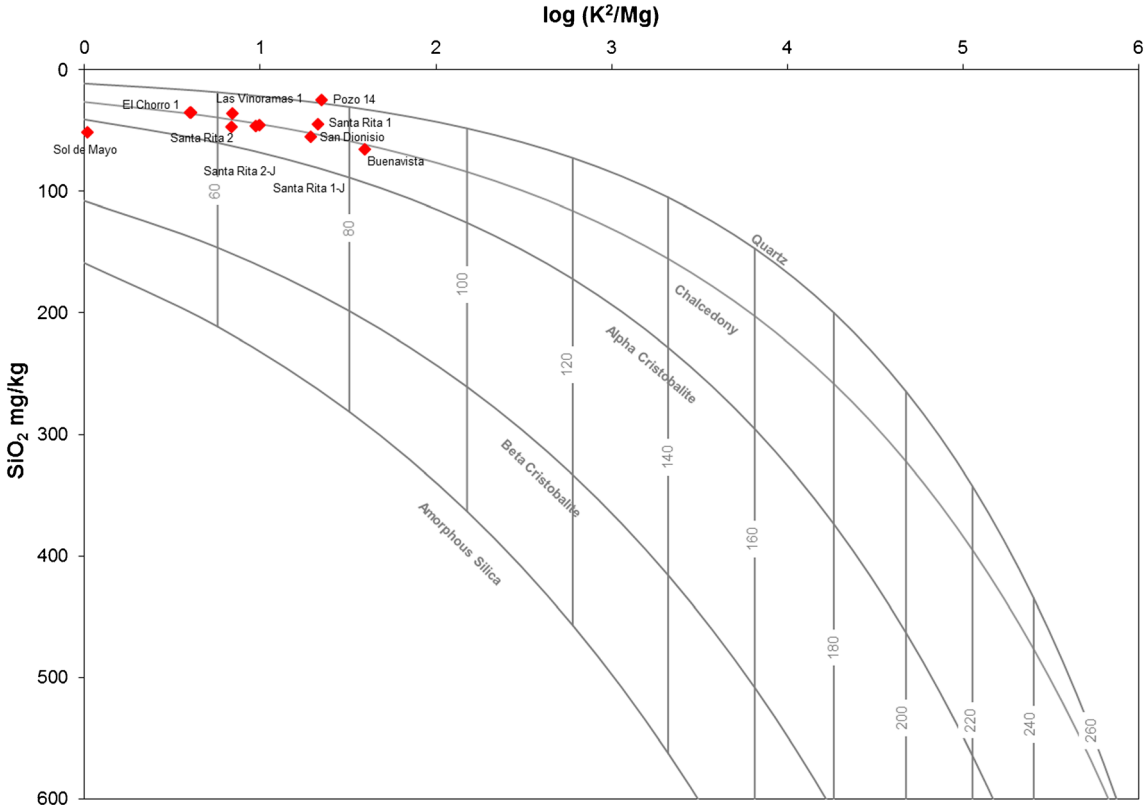

Fig. 11 The quartz geoindicator vs cations show samples mostly located on the equilibrium line for chalcedony to temperatures between 60 and 80 °C and moving into the field of amorphous silica

source maintains a temperature ranging from 71 to 115 °C according the SiO_2 geothermometer proposed by Verma and Santoyo (1997) which is taken as the most reliable for estimating the reservoir temperature due the notable less error in comparison with other SiO_2 geothermometers (Table 5). The calculated equilibrium temperatures indicate a low enthalpy geothermal system. In discrepancy, most of the hot springs studied for Baja California Sur have calculated geothermal systems with higher temperatures than 100 °C (Las Tres Virgenes, Loreto, Bahia Concepcion, Los Cabos). Geothermometers based on SiO_2 are considered as the most adequate to determine the equilibrium temperature system in the geothermal springs studied in this research. Cation exchange geothermometers presented very different temperatures, and the high values of error (Table 5) to be taken as valid for estimate temperatures are notable.

The ternary diagrams indicate that there is a fluid mixture which may correspond to a water steam-heated phase, where meteoric water dilutes the system. Li–B–Cl and HCO_3–Cl–SO_4 diagrams indicate a low-temperature ionic ratio and mixing with meteoric waters (Powell and Cumming 2010).

Regarding the incidence of numerous fractures, they may be allowing both the vertically and lateral flow. So, it is inferred that the hydrothermal system is controlled by an intricate network of fractures which allow a relatively fast influx of meteoric water. Convective processes and a change in the density water vapor phase allows ejecting the water to the surface through the shear zone generated by the FSJC. The FSJC is defined as tectonically active and is related to extensional Gulf Province which has a displacement of the peninsula of Baja California to the NW (Martínez-Gutiérrez and Sethi 1997; Fletcher et al. 2000; Oskin et al. 2001; Martín-Barajas 2000; Weber 2012; Busch et al. 2011; Dorsey and Umhoefer 2012). This displacement generates normal faults with fall into the E direction, segmented by lateral faults, where intense fracturing occurs. The main dynamic refers to an area with extension fractures (Weber 2012). Busch et al. (2011) infer, based on geophysic records, a depth between 1.6 and 2.7 km to half graben block. This suggests that probably some fractures and the FSJC can be continued until at least 1000 m in depth, because granitic rocks have a high order of heat diffusion so that these can be influenced by a strong heat transfer at depth from the high temperature zones of the Gulf of California to the BLC (Báncora-Alsina and Prol-Ledesma 2006). Based on these structural conditions, presumably, the heat could be generated due to the geothermal gradient, the friction component of movement of the active structural system, the heat transfer from the rock, and its implications by thermodynamic reactions.

Conclusions

At least six springs show clear influence from geothermal fluids: The Vinoramas, El Chorro, Santa Rita, Sol de Mayo, San Dionisio, and Buenavista. The hydrogeochemical characterization of the sites indicates that the thermal reservoir is up to the same that is generating heat water, which is manifested through the hot springs on the surface to the western area of the basin Santiago and one for the area Buenavista.

Temperatures between 71 and 115 °C (Buenavista; see Table 5) are estimated from silica geothermometer selected (Verma and Santoyo 1997) to characterize the geothermal system in the Santiago watershed.

The samples from Las Vinoramas, El Chorro, Santa Rita, Sol de Mayo, and San Dionisio belong to the sodium bicarbonate type with low mineralization. A mixture of water–steam heated, with a component of surface water, would be causing a decrease in mineralization; as well as caloric loss to the water flow during the rise from geothermal system. This effect would be much more dynamic for the Sol de Mayo than to El Chorro and Santa Rita springs.

A very low to low enthalpy geothermal system is recharged by the meteoric water in the Santiago watershed. The thermal springs with relatively low mineralization and high pH do not indicate water–rock interaction as their main factor for mineralization, but there may exist an important dilution due a mixing with meteoric water in a steam–water phase; moreover, the EF results show an external enrichment source due to the water–rock interaction. The geotermalism could be linked to FSJC as active fault where the geothermal gradient, the heat flow, which is higher than in average of this area (Báncora-Alsina and Prol-Ledesma 2006), and heat transfer by diffusion represent the main factors to build the heat source.

Of special interest is the Buenavista spring, which is located far from structural zone FSJC. This spring represents similar characteristics in respect to other geothermal manifestations found along the east and west margin of the peninsula. A secondary listric fault in the BLC area could be the heat source for this spring.

For all analyzed sites, any volcanic or direct magmatic component is discarded. The geothermal system is of low enthalpy so that the potential to generate electricity is reduced; UABC (2011) predicts that it is possible to generate electricity for local consumption. Due to new areas with thermal manifestations documented in this study, it is recommended to determine the energy that could provide the system in the Santiago area. Thermal water could be used not only for power generation at small scale but also with respect to other activities as direct use: agricultural industry, pharmaceutical, food, and tourism. Some of the springs are located within a protected area created by the Mexican government (Biosphere Reserve of the Sierra La Laguna).

Br/Cl and B/Cl ratios show that the source corresponds to water with a marine origin for this elements where dilution due to evaporation is observed. The enrichment factors indicate a notable impact of F and B in the aqueous system from interaction with the rocks. This enrichment is atributed to the lithological composition of the granitic batholith.

A different, but not independent geothermal system, was found in the Buenavista area, where the thermal water is affected due to mixture with seawater. An intricate network of fractures maintains the hydrothermal system and would be strongly linked to geological structures that exist in the BLC.

Acknowledgments CONACYT (Mexican Sciences and Technology National Council) scholarship grant No. 309028.

UABCS (Autonomous University of Baja California Sur) for fund grants.

Geology and Marine Biology departments of UABCS.

Geology Institute of San Luis Potosí and Engineering Faculty of Earth Science of the Autonomous University of San Luis Potosí, México.

References

Aranda-Gómez JJ, Pérez-Venzor JA (1989) Stratigraphy of the crystalline complex in the region of Todos Santos, Baja California Sur. Univ. Nal. Auton. Mexico Instituto de Geología Revista 8(2):149–170 (In spanish)

Aranda-Gómez JJ, Henry C, Luhr D (2000) Post-Paleocenic tectonomagmatic evolution of Sierra Madre Occidental and south portion of the basin and range province, Mexico. Bol Soc Geol Mex LIII:59–71 (In spanish)

Arango-Galván C, Prol-Ledesma RM, Torres-Vera MA (2015) Geothermal prospects in the Baja California Peninsula. Geothermics 55:39–57. doi:10.1016/j.geothermics.2015.01.005

Arnórsson S (2000a) Isotopic and chemical techniques in geothermal exploration, development and use. Sampling methods, data handling and interpretation. International Atomic Energy Agency, Vienna

Arnórsson S (2000b) The quartz and Na/K geothermometers. I. New thermodynamic calibration. Proceedings, World Geothermal Congress, Japan. 929–934.

Báncora-Alsina C, Prol-Ledesma RM (2006) Heat flow map of the Peninsula and Gulf of California. Geos 26(1):22 (In spanish)

Bear J, Alexander H, Cheng D, Sorek S, Ouazar D, Herrera I (2013) Seawater intrusion in coastal aquifers: concepts, methods and practices. Volumen 14. Theory and applications of transport in porous media series. Springer Science & Business Media.

Bertani R (2016) Geothermal power generation in the world 2010–2014 update report. Geothermics, Vol 60:31–43. doi:10.1016/j.geothermics.2015.11.003

Bravo-Pérez JR, (2002) Segmentation of the San José del Cabo Fault and its relation with the tectonostratigraphic evolution of the San José del Cabo Basin, Baja California Sur, Mexico. Thesis. Centro de Investigación Científica y de Educación Superior de Ensenada. Ensenada, Baja California. (In spanish)

Busch MM, Arrowsmith JR, Umhoefer PJ, Coyan JA, Maloney SJ, Martínez-Gutiérrez G (2011) Geometry and evolution of rift-margin, normal-fault-bounded basins from gravity and geology, La Paz–Los Cabos region, Baja California Sur. México: Lithosphere 3(2):110–127. doi:10.1130/L113.1

Canet C, Prol-Ledesma RM, Torres-Alvarado I, Gilg HA, Villanueva RE, Lozano R (2005) Silica-carbonate stromatolites related to coastal

hydrothermal venting in Bahía Concepción, Baja California Sur, Mexico. Sediment Geol 174:97–113
Cardona A, Carrillo-Rivera JJ, Huizar-Álvarez R, Granel-Castro E (2004) Salinization in coastal aquifers of arid zones: an example from Santo Domingo, Baja California Sur, Mexico. Environ Geol 45:350–366
Carrillo-Chávez A, Drever JI, Martínez M (2000) Arsenic content and groundwater geochemistry of the San Antonio-El Triunfo, Carrizal and Los Planes aquifers in southernmost Baja California, Mexico. Environ Geol 39(11):1295–1303
CLICOM (2015) SMN daily weather data through CICESE web platform. http://clicom-mex.cicese.mx. Accessed 16 Nov 2015 (In Spanish)
CONAGUA (2014) Hurricane Odile review. Mexico National Meteorological Service. http://smn.cna.gob.mx/tools/DATA/Ciclones%20Tropicales/Ciclones/2014-Odile.pdf. Accessed 2 Nov 2015 (In Spanish)
CONAGUA (2015) Update of the annual average availability of water in the Santiago aquifer (0320), Baja California Sur. DOF 20-04-2015. Mexico. 22. (In spanish)
Díaz SC, Salinas-Zavala CA, Hernández-Vázquez S (2008) Variability of rainfall from tropical cyclones in northwestern Mexico and its relation to SOI and PDO. Atmosfera 21(2):213–223
Díaz-González L, Santoyo E, Reyes-Reyes J (2008) Three new improved Na/K geothermometers using computational and geochemiometrics tools: application to the temperature prediction of geothermics systems. Revista Mexicana de Ciencias Geológicas 25(3):465–482 (In spanish)
Dorsey RJ, Umhoefer PJ (2012) Influence of sediment input and plate-motion obliquity on basin development along an active oblique-divergent plate boundary: Gulf of California and Salton Trough. In: Busby C, Azor A (eds) Tectonics of sedimentary basins: recent advances. Wiley, Chichester. doi:10.1002/9781444347166.ch10
Dorsey RJ, Umhoefer PJ, Ingle JC, Mayer L (2001) Late Miocene to Pliocene stratigraphic evolution of northeast Carmen Island, Gulf of California: implications for oblique-rifting tectonics. Sediment Geol 144:97–123
Fletcher JM, Munguía L (2000) Active continental rifting in southern Baja California, Mexico: implications for plate motion partitioning and the transition to seafloor spreading in the Gulf of California. Tectonics 19(6):1107–1123. doi:10.1029/1999TC001131
Fletcher JM, Khon BP, Foster DA, Gleadow AJW (2000) Heterogeneous cooling and exhumation of the Los Cabos Block, southern Baja California evidence from fission track thermochronology. Geology 28:107–110
Fletcher JM, Pérez-Venzor JA, Gonzalez-Barba G, Aranda-Gomez JJ (2003) Ridge-Trench interactions and the ongoing capture of the Baja California microplate-new insights from the southern Gulf extensional province, in Geologic transects acroos Cordilleran Mexico, Guidebook for the field trips of the 99th Geological Society of America Cordilleran Section Anual Meeting, Publicación Especial 1, Field trip 2, 13–31
Fournier RO (1977) Chemical geothermometers and mixing models for geothermal systems. Geothermics 5:41–50
Fournier RO (1979) A revised equation for the Na/K geothermometer. Geothermal Resources Council Trans 3:221–224
Fournier RO, Potter RW II (1982) A revised and expanded silica (quartz) geothermometer. Geothermal Resources Council Bulletin 11:3–12
Frizzell VA (1984) The geology of Baja California peninsula: an introduction. In: Frizzell VA Jr (ed) Geology Baja California Peninsula. Field trip guidebook. Society of Economic Paleontologists and Mineralogists, Pacific Section, San Diego v. 39, 1–8
Gastil G, Krummenacher D, Douppont J, Bushee J, Jensky W, Barthelmy D (1976) The batholithic zone of the south of California and the western of Mexico. Bol Soc Geol Mex 37:84–90 (In Spanish)
GEA (2016) Geothermal Energy Association. Annual U.S & Global Geothermal Power Production Report. March
Giggenbach WF (1988) Geothermal solute equilibria. Derivation of Na-K-Mg-Ca. Geochim Cosmochim Acta 52(12):2749–2765
Giggenbach WF, Goguel RL (1989) Collection and analysis of geothermal and volcanic water and gas discharges. DSIR report CD 2401, 4th ed. Pentone, New Zealand
González-Abraham A, Fagundo-Castillo JR, Carrillo-Rivera JJ, Rodríguez-Estrella R (2012) Geochemical groundwater flow systems in sedimentary and volcanogenics rocks of Loreto, BCS, Mexico. Bol Soc Geol Mex 64(3):319–333 (In spanish)
González-Ruíz L, González-Partida E, Garduño-Monroy VH, Martínez L, Pironon J, Díaz-Carreño EH, Yáñez-Dávila David, Romero Rojas W, Romero-Rojas MC (2015) Distribution of geothermal anomalies in Mexico: a useful guide in geothermal prospecting. RIIIT 2:1–27 (In Spanish)
Gunnarsson I, Arnórsson S (2000) Amorphous silica solubility and the thermodynamic properties of H4SiO4 in the range of 0 to 350 C at P sat. Geochim Cosmochim Acta 64(13):2295–2307
Hausback BP (1984) Cenozoic volcanic and tectonic evolution of Baja California Sur, Mexico. In: Frizzel VA Jr (ed) Geology of the Baja California Peninsula: Pacific Section Society Economic Paleontologists and Mineralogists, v. 39, p 219–236
Hill MN (2005) The composition of sea-water comparative and descriptive oceanography, volumen 2. The sea: ideas and observations on progress in the study of the seas. The global coastal ocean. Harvard University Press
Iglesias ER, Torres-Rodríguez RJ, Martínez-Estrella JI, Reyes-Picasso N (2011) Summary of the 2010 assessment on medium to low temperature geothermics resources in Mexico. Geotermia 24(2) (In Spanish)
Kimbrough DL, Smith DP, Mahoney JB, Moore TE, Grove M, Gastil RG, Ortega-Rivera A (2001) Forearc-basin sedimentary response to rapid Late Cretaceous batholith emplacement in the peninsular ranges of southern and Baja California. Geology 29:491–494
Lee J, Miller MM, Crippen R, Hacker B, Vazquez JL (1996) Middle Miocene extension in the Gulf Extensional Province, Baja California: evidence from the southern Sierra Juarez. Geol Soc Am Bull 108(5):505–525
López-Sánchez A, Báncora-Alsina C, Prol-Ledesma RM, Hiriart G (2006) A new geothermal resource in Los Cabos, Baja California Sur, México. Proceedings 28th New Zealand Geothermal Workshop. S3–6.
Lugo-Hubp J (1990) The relief of the Mexican Republic. Univ. Nal. Autón. México. Instituto de Geología. Revista 9(1):82–111. (In Spanish)
Martín-Barajas A (2000) Vulcanism and extensión of the extensional province of the gulf of California. Bol Soc Geol Mex 53:72–83 (In Spanish)
Martínez-Gutiérrez G, Sethi PS (1997) Miocene-Pleistocene sediments within the San José del Cabo Basin, Baja California Sur, México. In: Johnson ME, Ledesma-Vázquez J (eds) Pliocene carbonates and relates facies flanking the Gulf of California, Baja California, México: Geological Society of America, Special paper, 318, p 141–166
Martínez-Gutiérrez G, Díaz-Gutiérrez JJ, Cosío-González O (2010) Morphometric analysis in the watershed San José del Cabo, B.C.S. Mexico: an approximation in the identification of potential catch areas. Revista Mexicana de Ciencias Geológicas 27(3):581–592 (In Spanish)
Maya-González R, Gutiérrez-Negrín LCA (2007) Geothermal resources for electricity generation in Mexico. Rev Dig Univ (UNAM) 8(12). (in spanish)
McCloy C (1984) Stratigraphy and depositional history of the San Jose del Cabo trough, Baja California Sur, México. In: Frizzell VA Jr (ed) Geology of the Baja California Peninsula, field trip guidebook: San Diego, Society of Economic Paleontologists and Mineralogists, Pacific Section, v. 39, 237–267

Nieva D, Nieva R (1987) Developments in geothermal energy in Mexico. Part twelve: a cationic geothermometer for prospecting of geothermal resources. Heat Recov Syst 7:243–258

NMX-AA-003 (1980) Sewage wáter. Sampling. Secretaría de Economía. Diario Oficial de la Federación. 25 de Marzo de 1980. (In Spanish)

NMX-AA-014 (1980) Receiving bodies. Sampling. Secretaría de Economía. Diario Oficial de la Federación. 25 de Marzo de 1980. (In Spanish)

Okay C, Akkoyunlu BO, Tayanc M (2002) Composition of wet deposition in Kaynarca, Turkey. Environmental Polution 118:401–410

Ordaz-Méndez CA, Flores-Armenta MC, Ramírez-Silva GR (2011) Geothermic potential of the Mexican Republic. Geotermia Revista Mexicana de Geoenergía 24(1):58–59 (In spanish)

Oskin M, Stock J, Martin-Barajas A (2001) Rapid localization of Pacific-North America plate motion in the Gulf of California. Geology 29(5):459–462

Pantoja-Alor J, Carrillo-Bravo J (1966) Geological sketch of the Santiago-San Jose del cabo region, Baja California. Boletín de la Asociación Mexicana de Geólogos Petroleros 58:1–14 (In spanish)

Pérez-Venzor JA (2013) Geological-geochemical study of the eastern edge of the Los Cabos Block, Baja California Sur, México. Dissertation. UNAM. México. (In spanish)

Piper AM (1944) A graphic procedure in the geochemical interpretation of water analyses. Trans Am Geophys Union 25:914–924

Portillo-Pineda R (2012) Structure and kinematics of the opening of the Gulf of California, through physical experiments of crustal and lithospheric extensión. Thesis. Universidad Nacional Autónoma de méxico. (In Spanish)

Portugal E, Birkle P, Barragan RM, Arellano VM, Tello HE, Tello LM (2000) Hydrochemical isotopic and hydrogeological conceptual model of the Las tres Vírgenes geothermal field, Baja California Sur, México. J Volcanol Geotherm Res 101:223–244

Powell T, Cumming W (2010) Spreadsheets for geothermal water and gas geochemistry. In: Geothermometry, 2010, Proceedings, Thirty-Fifth Workshop on Geothermal Reservoir Engineering, Stanford University, Stanford, California, SGP-TR-188

Prol-Ledesma RM, Canet C, Torres-Vera MA, Forrest MJ, Armienta MA (2004) Vent fluid chemistry in Bahía Concepción coastal submarine hydrothermal system, Baja California Sur, Mexico. J Volcanol Geotherm Res 137:311–328

Prol-Ledesma RM, Dando PR, De Ronde CEJ (2005) Special issue on shallow-water hydrothermal venting. Chem Geol 224:1–4

Ramírez-Guzmán A, Taran Y, Armienta MA (2004) Geochemistry and origin of high-pH thermal springs in the Pacific coast of Guerrero, Mexico. Geofisica internacional 23(3):415–425

Rosales-Ramírez TY, Weber B, Carrera-Muñoz M (2011) Chemical and isotopic recognition of the La Paz coastal aquifer, BCS. Evaluation of posible seawater intrusión. XXI Congreso nacional de geoquímica (INAGEQ 2011). 172. (In spanish)

Schaaf P, Bohnel JJ, Pérez-Venzor JA (2000) Pre-Miocene palaeogeography of the Los Cabos Block, Baja California Sur: geochronological and palaeomagnetic constraints, Elsevier. Tectonophysics 318:53–69

Sedlock RL (2003) Geology and tectonics of the Baja California Peninsula and adjacent areas. In: Johnson SE, Paterson SR, Fletcher JM, Girty GH, Kimbrough DL, Martin-Barajas A, (eds) Tectonic evolution of Northwestern Mexico and Southwestern U.S.A. Geological Society of America, Boulder, Special Paper 374, p 1–42

Sedlock RL, Ortega-Gutiérrez F, Speed RC (1993) Tectonostratigrafic terranes and tectonic evolution of México: Geological Society of America, Special Paper 278, p 153

SMWW (1999) Standars of examination methods for water and wastewater, published by APHA, AWWA and WPCF, 20th edn.

Stock JM, Hodges KV (1989) Pre-Pliocene extension around the Gulf of California and the transfer of Baja California to the Pacific plate. Tectonics 8(1):99–115. doi:10.1029/TC008i001p00099

Sutherland FH, Kent GM, Harding AJ, Umhoefer PJ, Driscoll NW, Lizarralde D, Fletcher JM, Axen GJ, Holbrook WS, González-Fernández A, Lonsdale P (2012) Middle Miocene to early Pliocene oblique extension in the southern Gulf of California. Geosphere 8:752–770. doi:10.1130/GES00770.1

Taran Y, Morán-Centeno D, Inguaggiato S, Varley N, Luna-González L (2013) Geochemistry of thermal springs and geodynamics of the convergent Mexican Pacific margin. Chem Geol 339:251–262

Tello-Hinojosa E, Verma MP, González-Partida E (2005). Geochemical characteristics of reservoir fluids in the Las Tres Virgenes, BCS, México. Proceedings World Geothermal Congress 2005. Antalya, Turkey

Torres-Rodríguez V (2000) Geothermal chart of México scale 1:2,000, 000, Proceedings World Geothermal Congress 2000, pp 1867–1870

UABC (2011) Evaluation of low enthalpy geothermal resources Baja California, México. Universidad Autónoma de Baja California. Reporte final. Comisión Reguladora de energia (CRE). (In spanish)

Umhoefer P, Dorsey R, Willsey S, Mayer L, Renne P (2001) Stratigraphy and geochronology of the Comondu group near Loreto, Baja California Sur. Mexico: Sedimentary Geology 144:125–147. doi:10.1016/S0037-0738(01)00138-5

Umhoefer PJ, Mayer L, Dorsey RJ (2002) Evolution of the margin of the Gulf of California near Loreto, Baja California Peninsula, Mexico. Geol Soc Am Bull 114:849–868

US-EPA/600/4-79-020 (1983). Methods for chemical analysis of water and wastes. United States, Environmental Protection Agency, Environmental Monitoring and Support Laboratory. 26 W St. Clair Street, Cincinnati, OH 45268

Vengosh A (2003) Salinization and saline environments. Treatise on geochemistry. Elsevier Ltd. Vol., 9, p 333–365

Verma MP (2015) Chemical and isotopic geothermometers to estimate geothermal reservoir temperature and vapor fraction. Proceedings World Geothermal Congress. Melbourne, Australia, 19–25 April 2015

Verma SP, Santoyo E (1997) New improved equations for Na/K, Na/Li and SiO2 geothermometers by outlier detection and rejection. J Volcanol Geotherm Res 79(1–2):9–24

Verma SP, Pandarinath K, Santoyo E, González-Partida E, Torres-Alvarado IS, Tello-Hinojosa E (2006) Fluid chemistry and temperaturas prior to exploitation at the Las Tres Virgenes geotermal field, México. Geothermics 35:156–180

Verma SP, Pandarinath K, Santoyo E (2008) SolGeo: a new computer program for solute geothermometers and its application to Mexican geothermal fields. Geothermics 37(6):597–621. doi:10.1016/j.geothermics.2008.07.004

Vermette SJ, Drake JJ, Landsberger S (1988) Intra-urban precipitation quality: Hamilton, Canada. Water Air Soil Pollut 38:37–53

Villanueva-Estrada RE, Prol-Ledesma RM, Torres-Alvarado IS, Canet C (2005) Geochemical modeling of a shallow submarine hydrothermal system at Bahía Concepción, Baja California Sur, México in Proceedings World Geothermal Congress: Antalaya

Weber J (2012) Paleomagnetic quantification of neogene block rotations within an active transtensional plate boundary, Baja California Sur, Mexico. Dissertation, LMU München: Fakultät für Geowissenschaften

Wurl J, Hernández-Morales P, Imaz-Lamadrid MG (2009) Water quality in the Santiago watershed, Baja California Sur, Mexico. Hydrogeochemical study and statistical analysis. XIX Congreso Nacional de Geoquímica INAGEQ, Vol. 15, No. 1, Septiembre 2009

Wurl J, Mendez-Rodriguez L, Acosta-Vargas B (2014) Arsenic content in groundwater from the southern part of the San Antonio-El Triunfo mining district, Baja California Sur, Mexico. J Hydrol 518:447–459